Industrial Crops & Products 130 (2019) 273–284

Contents lists available at ScienceDirect

Industrial Crops & Products

journal homepage: www.elsevier.com/locate/indcrop

High-pressure ultrasonic-assisted extraction of polysaccharides from *Mentha haplocalyx*: Structure, functional and biological activities

Guangjing Chen[a,b,c], Chuchu Fang[a,b,c], Xuhui Chen[a,b,c], Zhirong Wang[a,b,c], Min Liu[a,b,c], Jianquan Kan[a,b,c,*]

[a] College of Food Science, Southwest University, 2 Tiansheng Road, Beibei, Chongqing 400715, PR China
[b] Laboratory of Quality & Safety Risk Assessment for Agro-products on Storage and Preservation (Chongqing), Ministry of Agriculture and Rural Affairs of the People's Republic of China, Chongqing 400715, PR China
[c] Chinese-Hungarian Cooperative Research Centre for Food Science, Chongqing 400715, PR China

ARTICLE INFO

Keywords:
Mentha haplocalyx
Polysaccharides
High-pressure ultrasonic-assisted extraction
Physicochemical characterization
Functional property
Antioxidant activity

ABSTRACT

In the present study, *Mentha haplocalyx* polysaccharides (MHP) were extracted using a high-pressure ultrasound-assisted extraction (HUAE) method. Response surface methodology (RSM) was used to select the conditions for the extraction of MHP; this method predicted that optimized extraction is obtained using 300 W of ultrasonic power, an extraction temperature and time of 70 °C and 28 min, respectively, and 29 mL of water for every gram of raw material used in the extraction. Results showed that MHP mainly contained neutral sugar (69.09 ± 0.81%), uronic acid (3.89 ± 0.14%), and protein (7.97 ± 0.42%). Specifically, MHP was comprised of mannose, rhamnose, glucuronic acid, galacturonic acid, glucose, galactose, and arabinose with molar percentages of 2.13, 0.89, 1.14, 3.79, 39.3, 44.85, and 7.89%, respectively, and with an average molecular weight of 59.58 kDa for its major component (accounting for 66.20% of MHP). Functional analyses demonstrated that MHP exhibits favorable oil-holding capacity, foaming qualities, emulsifying capacity, hygroscopicity, and moisture retention capacity. The results obtained from the X-ray diffraction pattern and rheological measurements confirmed a semi-crystalline nature of the sample and shear thinning behavior of MHP, respectively. Additionally, *in vitro* antioxidant activity experiments suggested that MHP exhibits strong DPPH and hydroxyl radical scavenging activities and considerable reducing power. The results presented herein have larger implications for the use of MHP as a functional additive in the food and pharmaceutical industries.

1. Introduction

Over the last few decades, plant-derived polysaccharides have received much attention because of their pharmacological properties such as antioxidant, anti-tumor, immunomodulatory, anti-inflammatory, anti-diabetic, anti-viral and prebiotic behaviors (Chen et al., 2017a, 2017b; Chen et al., 2018a; Dong et al., 2011; He et al., 2016; Sun and Zhou, 2012). These natural products are particularly attractive due to their lower toxicity and decreased side effects relative to synthetic antioxidants (Liao et al., 2015). Moreover, natural plant-sourced polysaccharides are of interest in functional food, biomedical and pharmaceutical industries due to their strong hydrophilic character, ideal rheological properties, and their favorable functional properties such as gelling, foaming, emulsifying, and thickening (McClements et al., 2017; Wang et al., 2018; Zhu et al., 2017). However, a challenge associated with the study of polysaccharides is derived from the structural diversity of the polysaccharides extracted from different raw materials, including differences in molecular weight, monosaccharide composition, and conformation of the glycosidic bonds, which are all closely correlated to their bioactivities and functional properties (Funami et al., 2011; Zhu et al., 2016). Characterization of the polysaccharides isolated from a new raw material, in terms of structural characteristics, functional properties and biological activities, is therefore essential in assessing their potential for applications in health care, the food industry, and materials science.

Mentha haplocalyx Briq., a perennial plant belonging to the family *Lamiaceae*, is a significant economic crop produced in the provinces of Southwest China, which is widely used in food, cosmetics, and medicine

Abbreviations: HUAE, high-pressure ultrasound-assisted extraction; MHP, the *Mentha haplocalyx* polysaccharides

* Corresponding author at: College of Food Science, Southwest University, 2 Tiansheng Road, Beibei, Chongqing 400715, PR China.
E-mail addresses: gjchen1989@126.com (G. Chen), 1362377011@qq.com (C. Fang), 2269535890@qq.com (X. Chen), 1059544916@qq.com (Z. Wang), 1595484556@qq.com (M. Liu), kanjianquan@163.com (J. Kan).

https://doi.org/10.1016/j.indcrop.2018.12.086
Received 2 October 2018; Received in revised form 13 December 2018; Accepted 27 December 2018

(Park et al., 2016). For example, fresh *Mentha haplocalyx* oil extracted from the leaves of *M. haplocalyx* Briq. is a common treatment in Chinese folk medicine, used for to treat halitosis, as well as problems with the procreation and digestive systems (She et al., 2012). The use of *M. haplocalyx* in medicine is further supported by modern pharmacological research, which has identified a wide range of bioactive properties of *M. haplocalyx,* including anti-oxidant, anti-inflammatory, anti-tumor, anti-microbial, anti-allergenic, anti-viral, gastrointestinal protective and hepatoprotective behaviors (Cao et al., 2011; Zheng and Wang, 2001). A diverse collection of materials has been isolated from *M. haplocalyx*, including essential oils, polyphenolic acids, flavonoids, and monoterpenoids (Liu et al., 2005; Mimica-Dukic and Bozin, 2008; Wei et al., 2003). Much of the research to date has focused on volatile components isolated from *M. haplocalyx*, such as essential oils and small molecules (Cao et al., 2011; Chen et al., 2017a, 2017b; Dong et al., 2015). However, little information is available regarding the structural characteristics, functional property, and biological activity of the polysaccharides extracted from *M. haplocalyx*.

Extraction of polysaccharides is typically carried out using water or aqueous organic solvents. However, the extraction of polysaccharides from plants is complicated by the complex polymers of the cell wall, which can prevent extraction of polysaccharides in their active form (Wijesinghe and Jeon, 2012). Several strategies have emerged in recent years to improve this extraction process, such as ultrasonic-assisted extraction (Chen et al., 2018b), microwave-assisted extraction (Chen et al., 2017a, 2017b), enzyme-assisted extraction (Yang et al., 2017), accelerated solvent extraction (Chen et al., 2018a), pressurized water extraction (Xu et al., 2016), and ultrahigh pressure extraction (Chen et al., 2014). These extraction techniques present advancement in terms of simplified procedures, improved efficiency, lower solvent volume, and higher yield. Of the modified extraction procedures, high-pressure ultrasonic-assisted extraction (HUAE), a technique that couples high-pressure- and ultrasonic-assisted extraction, shows great promise. The extraction efficiency of polysaccharides can be enhanced by HUAE whose ultrasonic cavitation, mechanical effects and catalytic action would accelerate the release, diffusion, and dissolution of intracellular substances. The use of HUAE can promote solvent penetration into the cell matrix, and consequently the release of intracellular products in two ways: (1) the application of high pressure to the raw material while subjecting it to ultrasonic waves creates shear forces that accelerate disruption of cell walls and produce cavitation bubbles (Liu et al., 2014a, 2015), and (2) the high pressure increases the solubility of target compounds, and decrease the solvent viscosity and surface tension (Lou et al., 1997). While HUAE has been applied to the extraction of biologically active substances (Liu et al., 2014a, 2015), the application of this technique to *M. haplocalyx* for the extraction of polysaccharides has yet to be reported. We hypothesize that the *M. haplocalyx* polysaccharides extracted using HUAE may possess favorable antioxidant capacity and functional properties, thereby developing as a functional component or antioxidant agent in the food, pharmaceutical or cosmetic industries.

To this aim, the work reported herein establishes an optimized method for the isolation of polysaccharides from *M. haplocalyx* (MHP) via HUAE. The structural characteristics and physicochemical properties of the isolated MHP were then determined using colorimetry, HPGPC, HPLC, FT-IR, XRD, and TGA. Finally, investigation of the functional properties and antioxidant activity of MHP *in vitro* has larger implications in the potential applications of the polysaccharides from *M. haplocalyx*.

2. Materials and methods

2.1. Materials and reagents

The fresh stems and leaves of *M. haplocalyx* were acquired from Chengdu Maoyixiang Commercial and Trading Co. Ltd (Sichuan Province, China) in September 2017. The samples were dried naturally, then ground into powders, sifted through a 60 mesh sieve, pretreated with petroleum ether at room temperature for 8 h × 3, and then extracted with 95% ethanol at 60 °C for 4 h × 3 for removal of pigments, fats and monosaccharides. The residue was separated from the ethanol by vacuum filtration and dried in an air drying oven at 40 °C for 18 h. Finally, the dried residue was sealed in airtight plastic bags for storage prior to use.

The chemicals bovine serum albumin (BSA, A1933-1G), D-galacturonic acid (GalA, 92478-25MG), D-glucuronic acid (GlcA, G5269-10G), 1-phenyl-3-methyl-5-pyrazolone (PMP, M70800-100G), and diphosphopyridine nucleotide (NADH, 10107735001) were purchased from Sigma-Aldrich Chemical Co. (St. Louis, MO, USA). 3-phenylphenol (P0768), L-fucose (Fuc, F0065), L-rhamnose (Rha, R0013), L-arabinose (Ara, A0515), D-ribose (Rib, R0025), D-mannose (Man, M0045), D-galactose (Gal, G0008), D-glucose (Glc, G0048), D-xylose (Xyl, X0019), D-Lactose (Lac, L0008), 1,1-diphenyl-2-picrylhydrazyl (DPPH, D4313), phenazine methyl sulfate (PMS, P1872) and nitrotetrazolium blue chloride (NBT, D0844) were obtained from TOKYO Chemical Industry Co., Ltd. (Japan). Dialysis bag (molecular weight cut-off, 8,000–14,000 Da) was purchased from Beijing Solarbio Science & Technology Co., Ltd (Beijing, China). All other used chemicals were of analytical grade and purchased locally.

2.2. Polysaccharides extraction procedure

The high-pressure ultrasonic extraction system (CSGF-500 ml, Xian Taikang Bio-Technology Co. Ltd., China) in Fig. 1(a) composed of a high-pressure nitrogen gas bottle (HNB), a pressure reducing valve

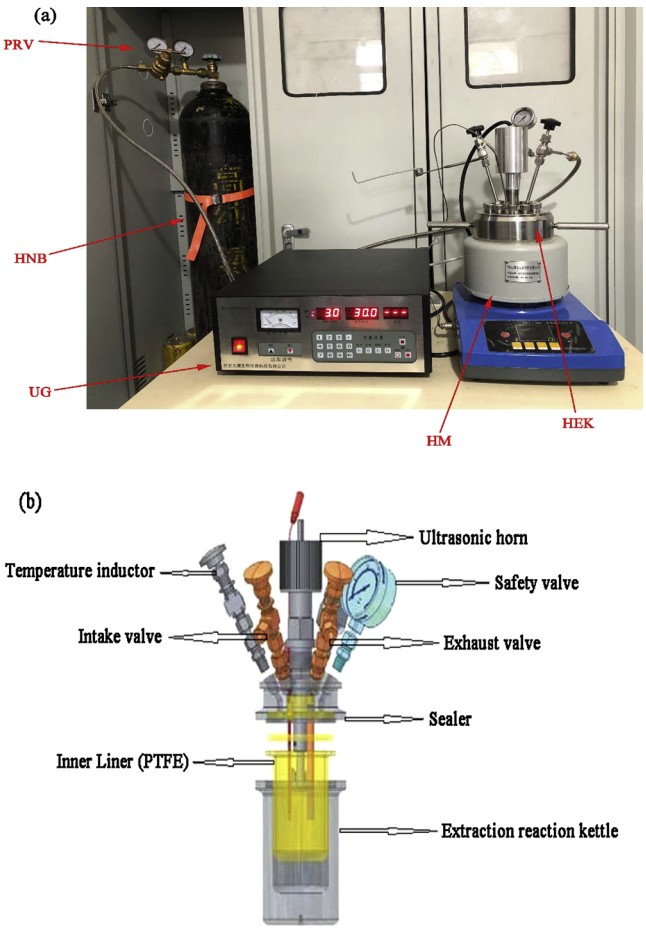

Fig. 1. The photo of the high-pressure ultrasonic extraction system (a) and the schematic of the high-pressure extraction reaction kettle (b).

Table 1
The Box–Behnken design (BBD) and the results for the yield of MHP.

No.	X_1 (ratio of water to raw material, g/mL)	X_2 (Ultrasonic power, W)	X_3 (Extraction temperature, °C)	X_4 (Extraction time, min)	Y (Extraction yield, %)
1	−1 (20)	−1 (250)	0 (70)	0 (30)	7.29
2	1 (30)	−1 (250)	0 (70)	0 (30)	7.48
3	−1 (20)	1 (350)	0 (70)	0 (30)	7.15
4	1 (30)	1 (350)	0 (70)	0 (30)	7.60
5	0 (25)	0 (300)	−1 (60)	−1 (20)	6.75
6	0 (25)	0 (300)	1 (80)	−1 (20)	6.38
7	0 (25)	0 (300)	−1 (60)	1 (40)	6.62
8	0 (25)	0 (300)	1 (80)	1 (40)	6.37
9	−1 (20)	0 (300)	0 (70)	−1 (20)	6.53
10	1 (30)	0 (300)	0 (70)	−1 (20)	7.78
11	−1 (20)	0 (300)	0 (70)	1 (40)	7.42
12	1 (30)	0 (300)	0 (70)	1 (40)	7.13
13	0 (25)	−1 (250)	−1 (60)	0 (30)	6.97
14	0 (25)	1 (350)	−1 (60)	0 (30)	7.14
15	0 (25)	−1 (250)	1 (80)	0 (30)	6.51
16	0 (25)	1 (350)	1 (80)	0 (30)	6.62
17	−1 (20)	0 (300)	−1 (60)	0 (30)	6.91
18	1 (30)	0 (300)	−1 (60)	0 (30)	6.76
19	−1 (20)	0 (300)	1 (80)	0 (30)	6.32
20	1 (30)	0 (300)	1 (80)	0 (30)	6.61
21	0 (25)	−1 (250)	0 (70)	−1 (20)	6.94
22	0 (25)	1 (350)	0 (70)	−1 (20)	7.59
23	0 (25)	−1 (250)	0 (70)	1 (40)	7.76
24	0 (25)	1 (350)	0 (70)	1 (40)	7.02
25	0 (25)	0 (300)	0 (70)	0 (30)	9.12
26	0 (25)	0 (300)	0 (70)	0 (30)	9.18
27	0 (25)	0 (300)	0 (70)	0 (30)	9.31
28	0 (25)	0 (300)	0 (70)	0 (30)	9.27
29	0 (25)	0 (300)	0 (70)	0 (30)	9.29

(PRV), an ultrasonic generator (UG), a heating mantle (HM), and a high-pressure extraction reaction kettle (HEK). The high-pressure extraction reaction kettle in Fig. 1(b) mainly consisted of an ultrasonic horn, an extraction reaction kettle, an intake valve, an exhaust valve and a safety valve. A 6-cm-long ultrasonic horn (6 mm, Φ) was used to generate ultrasound with different powers, which was immersed in extraction liquid with length of 2 cm.

Polysaccharides were extracted from *M. haplocalyx* using this system at a frequency of 40 KHz. The pretreated *M. haplocalyx* powders (5.0 g) were transferred to the high-pressure extraction reaction kettle, mixed with distilled water under the predesigned ratio of water to raw material, injected nitrogen gas using an HNB and pressurized to 10 MPa by adjusting the PRV. When the pressure achieved 10 MPa (monitored by the safety valve), the intake valve was closed and the extraction reaction kettle was held in the heating mantle to heat. The samples were extracted twice by HUAE using extraction conditions determined according to the Box-Behnken Design (BBD) for response surface methodology with 4 independent factors and 3 levels (Table 1). The appropriate range of values for each extraction parameter (ratio of water to raw material, ultrasonic power, and extraction temperature and time) was determined independently in accordance with single factor experiments (data not shown). The resultant extract was allowed to cool to room temperature, then centrifuged to remove particulate matter, and the supernatant was collected. The supernatant solutions from the two extractions were combined, concentrated to 1/4 of its original volume, and added to absolute ethyl alcohol (ratio of 3:1; v/v) overnight at 4 °C to form a precipitate. The mixture was centrifuged to facilitate isolation of the precipitate, which was then washed with a combination of ethanol, acetone and anhydrous diethyl ether. The remaining precipitate was re-dissolved in distilled water at 50 °C and subjected to the Sevage method for deproteinization eight times (Sevag et al., 1938). The solution was then intensively dialyzed for 72 h (MWCO 8,000-14,000 Da). Finally, the retentate from the dialysis bag was gathered, centrifuged, concentrated, and lyophilized (Alpha 2-4 LSCplus, CHRIST, Germany) to obtain the desired *M. haplocalyx* polysaccharides (MHP). The MHP yield (%) was computed using the following equation:

$$MHPyield(\%, w/w) = \frac{weightofdriedMHP(g)}{weightofpretreatedM.\ haplocalyxpowder(g)} \times 100 \quad (1)$$

2.3. Chemical determination

The phenol–sulfuric acid method (Dubois et al., 1956), Coomassie brilliant blue method (Zor and Selinger, 1996), and *m*-hydroxybiphenyl method (Blumenkrantz and Asboe-Hansen, 1973) were performed to estimate the contents of neutral sugar, protein, and uronic acid, respectively. Total polyphenols were measured by the Folin–Ciocalteu method and calculated using gallic acid as standard (Yen and Hsieh, 1998). Additionally, the total flavonoids were determined as rutin equivalents according to the colorimetric method as described by Jia et al. (1999). AOAC method was used to assay the moisture content.

The monosaccharide composition analysis of MHP was achieved by PMP derivatization in HPLC analysis. In a vacuum-sealed tube, the MHP sample (10 mg) was hydrolyzed at 121 °C for 4 h in the presence of 4 M trifluoroacetic acid (TFA, 4 mL). Removal of excess TFA was completed using an azeotrope with methanol. After the hydrolysis, the hydrolyzed MHP solution was derivated with PMP following a procedure previously described by Chen et al. (2018a). The PMP-labeled derivatives of MHP were analyzed by HPLC (Agilent 1260 Series, Agilent Technologies, CA, USA) equipped with a Zorbax Eclipse Plus-C18 column (4.6 mm × 100 mm, 5 μm, Agilent, USA) and a UV-detector (250 nm) according to the following chromatographic conditions: column temperature, 30 °C; mobile phase, a mixture of phosphate buffered saline (0.025 M, pH 6.7) and acetonitrile (83:17, v/v); flow rate, 0.5 mL/min; injection volume, 5 μL. The monosaccharide standards were derived and analyzed by the same procedure as above.

2.4. Molecular weight analysis

The Molecular weight (M_w) of MHP was analyzed using high performance gel permeation chromatography (HPGPC) technique with dextran standards (5,000, 12,000, 25,000, 50,000, 150,000 and 270,000 Da, Sigma–Aldrich, St. Louis, MO, USA). The HPGPC analysis was performed by an Agilent 1260system equipped with a refractive index detector (1260 RID, Agilent Technologies, CA, USA) using a TSK-Gel G4000 SWXL column (7.8 mm × 300 mm, Tosoh Biosep, Japan) at temperature of 30 °C. 10 μL of MHP (2 mg/mL) was eluted with 0.1 M KH_2PO_4 at a flow rate of 0.6 mL/min.

2.5. Fourier transform infrared (FT-IR) spectroscopic analysis

To prepare the infrared spectrum for MHP powder, the dried MHP (3 mg) was mixed with KBr powder (300 mg), then ground and pressed into pellets. By utilizing the Spectrum 100 spectrometer (PerkinElmer Co., USA), a FT-IR spectrum of the MHP was collected over the frequency range of 4000–400 cm^{-1}.

2.6. X-ray diffraction analysis

Powder X-ray diffraction (XRD) spectra of MHP were collected on an X'Pert3 Powder X-ray diffractometer (PANalytical, Nederland) equipped with a Cu anode. Data were collected under an applied voltage and current of 40 kV and 200 mA, respectively. Data were collected as 2θ scans, over the range of 5–80° with a scan rate of 0.5°/min.

2.7. Thermal property

The thermal stability of MHP was tested using thermogravimetric analysis (TGA). Using a DTG-60 A TGA analyzer (Shimadzu Co., Japan), the samples were heated from 25 to 700 °C, at a rate of 10 °C/min. Samples were held in a platinum crucible and maintained under a dynamic nitrogen atmosphere with a flow rate of 50 mL/min.

2.8. Functional properties assay

2.8.1. Water holding capacity (WHC) and oil holding capacity (OHC) assay

The WHC and OHC of MHP were evaluated by the method of a previous study described by Chen et al. (2018b).

2.8.2. Foaming qualities assay

The foaming qualities of MHP were assessed following a procedure previously described by Rezaei et al. (2016). MHP solutions (10 mL, concentrations 1%, 2%, 3%, 4% and 6%; w/v) were homogenized using a T10 homogenizer (IKA Co., Germany) for 60 s at room temperature (20 ± 2 °C) to incorporate air and induce foaming. The whipped samples were immediately subjected to tube volume measurement. The foaming capacity (FC) and foaming stability (FS) were measured by recording the foaming volume at t = 0 (initial foam volume) and 30 min (final foam volume), respectively. The FC and FS were computed according to the following equations:

$$FC(\%) = \frac{Initialfoamvolume}{Totalsuspensionvolume} \times 100 \quad (2)$$

$$FS(\%) = \frac{Finalfoamvolume}{Totalsuspensionvolume} \times 100 \quad (3)$$

2.8.3. Emulsion properties assay

The emulsion properties of MHP were measured using the method reported by Wang et al. (2018). To each MHP solution (10 mL, concentrations 1%, 2%, 3%, 4% and 6%; w/v) was added commercial soybean oil (3 mL), and the resultant mixture homogenized under the conditions described in Sections 2.8.2. Subsequently, each mixture was centrifuged at 1000*g* for 10 min and the emulsion capacity (EC) was computed by the following equation:

$$EC(\%) = \frac{Emulsionvolume}{Totalvolume} \times 100 \quad (4)$$

To test the emulsion stability (ES), each emulsion was heated to 80 °C for 30 min, then allowed to cool to approximately 25 °C, before being subjected to centrifugation at 1000*g* for 10 min. The ES was evaluated according to the following expression:

$$ES(\%) = \frac{Finalemulsionvolume}{Totalvolume} \times 100 \quad (5)$$

2.8.4. Hygroscopicity and moisture retention assay

The hygroscopicity (HP) and moisture retention (MR) of MHP were evaluated according to a protocol modified from the method reported by Zhu et al. (2017). To evaluate its HP, dried MHP (10 mg) was distributed in Petri dish and placed in a constant temperature and humidity chamber (LHS-150CLY, Shanghai keelrein instruments Co., Ltd., China) set to a relative humidity of 85% at 20 °C. The samples were weighed at regular intervals (4, 8, 12, 24, 36 and 48 h, respectively) and the HP was computed according to the following equation:

$$HP(\%) = \frac{(W_1 - W_0)}{W_0} \times 100 \quad (6)$$

where, W_0 represents the weight of the dried MHP and W_1 is the weight of MHP at the designated time interval.

Determination of MR was performed by comparing the weight of wet MHP samples to their weight after being heated to 40 °C in a desiccation chamber containing dried silica gel for a given time interval (4, 8, 12, 24, 36 and 48 h, respectively). The MR was computed by the following formula:

$$MR(\%) = \frac{weightofHMPforaperiodoftime}{initialweightofHMP} \times 100 \quad (7)$$

2.9. Rheological measurement

Steady-shear flow measurements of the MHP solutions at different concentrations were performed at 25 ± 0.1 °C, within 24 h after preparation in a TA Instruments AR550 rheometer (New Castle, USA), using a cone-and-plate geometry (40 mm in diameter and gap size of 0.5 mm) with duplication deliberations. Experimental flow curves were computed in the shear rate range of 0.01–1000 s^{-1}. The apparent viscosity (η)-shear rate ($\dot{\gamma}$) data were fitted with Cross (Eq. (8)), Carreau (Eq. (9)) and Power-law (Eq. (10)) models (Guo et al., 2017):

$$\eta = \eta_\infty + \frac{(\eta_0 - \eta_\infty)}{[1 + (a\dot{\gamma})^d]} \quad (8)$$

$$\eta = \eta_\infty + \frac{(\eta_0 - \eta_\infty)}{[1 + (c\dot{\gamma})^2]^p} \quad (9)$$

$$\eta = k \times \dot{\gamma}^{n-1} \quad (10)$$

Here, η is the apparent viscosity (Pa·s), η_0 is the zero shear viscosity (Pa·s), and η_∞ is the infinite shear rate apparent viscosity (Pa·s); $\dot{\gamma}$ represents the shear rate (s^{-1}); a and c denotes the time constants (s); k is the consistency index (Pa·s^n); d and p are rate indices; and n is the flow behavior index.

2.10. Antioxidant activity analysis of MHP

2.10.1. DPPH radical scavenging activity

The DPPH radical scavenging assay of MHP was performed following a previous study with slight modification (Chen et al., 2018a). In brief, DPPH solution (0.4 mM) was freshly prepared by dissolving with 100% methanol. 50 μL of different concentrations of the MHP in distilled water was thoroughly mixed with 100 μL of DPPH solution. The mixture was shaken well and kept in the dark at room temperature for 30 min, and then measured at 517 nm on a Synergy H1 Hybrid Multimode microplate reader (Biotek, USA). Vc was employed as a positive control. DPPH radical scavenging activity was computed by following equation:

$$Scavengingrate(\%) = \left(1 - \frac{A_1 - A_2}{A_0}\right) \times 100 \quad (11)$$

Where A_0 represents the absorbance of the control group (deionized water instead of the sample solution). A_1 is the absorbance of the sample reaction solution, and A_2 is the absorbance of the sample only (ethanol instead of DPPH solution).

2.10.2. Hydroxyl radical scavenging activity

The hydroxyl radical scavenging activity was estimated according to the reported method with necessary modification (Chen et al., 2018a). 50 μL of MHP with the different concentrations was incubated with 50 μL 1,10-phenanthroline (0.75 mM), 75 μL sodium phosphate buffer (0.15 M, pH 7.4), 50 μL $FeSO_4$ (0.75 mM) and 50 μL H_2O_2 (0.01%, v/v) at 37 °C for 60 min and the absorbance at 536 nm was determined by a microplate reader. The deionized water and Vc was used as the blank and positive control, respectively. Hydroxyl radical scavenging activity was calculated as follows:

$$Scavengingrate(\%) = \left(\frac{A_1 - A_0}{A_2 - A_0}\right) \times 100 \quad (12)$$

where A_0, A_1 and A_2 are the absorbance of the blank, sample and control solution (deionized water instead of H_2O_2 and sample solution), respectively.

2.10.3. Reducing power

The reducing power of MHP was evaluated according to the method described by previous study with minor modifications (Chen et al., 2018b). Chiefly, 50 μL of different concentrations of the MHP was mixed with 50 μL of 0.2 M phosphate buffer (pH 6.6) and 50 μL of 1% (w/v) potassium ferricyanide. The mixtures were incubated at 50 °C for 20 min before it was cooled at room temperature. Further, 50 μL of 10% (w/v) trichloroacetic acid and 25 μL of 0.1% (w/v) ferric chloride solution were added to the mixture. The mixture was shaken, and its absorbance was recorded at 700 nm against a blank sample after 10 min. Vc was used as a positive control.

2.10.4. Superoxide radical scavenging activity

The superoxide radical scavenging activity of MHP was measured in the NADH-NBT-PMS system with minor changes (Bi et al., 2013). Briefly, 50 μL of MHP with the different concentrations was added 50 μL of 300 μM NBT, 50 μL of 936 μM NADH, and 50 μL of 120 μM PMS in 100 mM phosphate buffer (pH 7.4) in sequence. After incubation at 25 °C for 5 min in the dark, the mixture was determined at 569 nm. Vc was used as a positive control. The scavenging superoxide radical activity was computed according to the Eq. (11). Where A_0 denotes the absorbance of the control group (deionized water instead of the sample solution). A_1 represents the absorbance of the sample group, and A_2 is the absorbance of the sample only (distilled water instead of NBT solution).

2.11. Statistical analysis

All the data were shown as the mean ± standard deviations, based on at least three independent experiments for each sample. The RSM design and data analysis was implemented using Design-Expert software (version 8.0.6.1, Stat-Ease, Inc, Minneapolis, USA).

3. Results and discussion

3.1. Optimization of HUAE conditions by BBD

Optimization of the HUAE procedure was determined as a function of the extraction yields of the MHP using the response surface methodology. The four independent factors of the BBD procedure for extraction of MHP were optimized over 29 runs. The Box-Behnken design matrix and results were provided in Table 1. The accuracy of the predicted model was assessed by comparison to a multiple regression analysis on the experimental data. The constructed model expresses the extraction yield of MHP (Y) according to the following second-order polynomial equation:

$$Y = 9.23 + 0.15X_1 + 0.014X_2 - 0.19X_3 + 0.029X_4 + 0.065X_1X_2 + 0.11X_1X_3 - 0.38X_1X_4 - 0.015X_2X_3 - 0.35X_2X_4 + 0.030X_3X_4 - 0.98X_1^2 - 0.84X_2^2 - 1.61X_3^2 - 1.07X_4^2 \quad (13)$$

The result and analysis of variance (ANOVA) for the fitted quadratic polynomial model of extraction yield of MHP is presented in Table 2. The F-value of 137.20 and p-value < 0.0001 determined for the overall model established its significance. The minimal divergence of the correlation coefficient (R^2 = 0.9928) from unity indicates that the model varies by only 0.72% from the empirical data. Moreover, the nearness of the R^2 and Adj-R^2 values, 0.9928 and 0.9855, respectively, to unity suggests a good fit between the predicted and experimental values (Liu et al., 2013); in other words, the model can be used to predict the MHP yield with reasonable accuracy. Moreover, as shown in Fig. 2A, a good fit between observed and predicted values was achieved. The lack of fit parameters F and p are small, 2.44 and 0.2018, respectively, indicating the divergence of the model from the experimental results is insignificant relative to experimental error (Gan and Latiff, 2011). Furthermore, a relatively low value of C.V. (1.56%) suggests a high precision and reliability of the method. The residuals from the least squares fit play a key role in checking model adequacy (Noshad et al., 2012). The adequacy of the model was further judged by normal probability plot of the residuals (Fig. 2B) that shows scatters along a straight line suggesting that the residuals follow a normal distribution pattern. As presented in Fig. 2C, residuals versus the predicted response plot displays a random distribution of residuals scatter, indicating that the variance of the original observation is constant for all values. All the plots (Figs. 2A, B and C) demonstrate the accuracy and applicability of BBD in designing optimized extraction for MHP.

The significance of each coefficient was also examined by the p-value obtained from an F-test ($p < 0.05$). A smaller p-value indicates a more significant contribution of the variable (González-Centeno et al., 2014). In particular, the X_1, X_3, X_1X_4, X_2X_4, X_1^2, X_2^2, X_3^2 and X_4^2 are the significant terms of the model ($p < 0.05$). By comparison of the F values, the order of impact of the four factors on the MHP yield is as follows: extraction temperature > ratio of water to raw material > extraction time > ultrasonic power. The truncated model to predict extraction yield was as given (Eq. (14)) considering the significance of the coefficients and the statistics of this model was presented in Table 3. The model p-value was found to be very low (< 0.0001), indicating this model is highly significant. The lack of fit of the model is not significant relative to the pure error (p-value = 0.2163 > 0.05), which suggests that the model represents the data in a satisfactory fashion.

$$Y = 9.23 + 0.15X_1 - 0.19X_3 - 0.39X_1X_4 - 0.35X_2X_4 - 0.98X_1^2 - 0.84X_2^2 - 1.61X_3^2 - 1.07X_4^2 \quad (14)$$

Their three-dimensional response surface could vividly portray the relationship between the independent variables and the response. To build the 3D surface plots, two of variables were plotted over the experimental range, while the remaining variables were fixed at zero. It was observed from Fig. 3A that MHP yield increased with the ratio of water to raw material from 20 mL/g to 25 mL/g, and slowly decreased afterwards. This is probably because a higher ratio of water to raw material prolonged the distance of diffusion towards the interior tissues and caused a little loss during production collection (Ying et al., 2011). MHP yield reached a peak value at 300 W, whereas it declined over 300 W. The 3D surface plot in Fig. 3B illustrated that the connection between the ratio of water to raw material and extraction temperature was significant and was correspond with the result in Table 2. According to the model, the yield of MHP initially increased with an increase in the ratio of water to raw material, but then decreased after a certain threshold was reached. A similar trend was observed in response to temperature perturbation; the predicted yield of MHP increased rapidly with increasing extraction temperature over the range of 60 °C to 69 °C, but then proceeded to decline rapidly as the temperature rose to 80 °C (Fig. 3F). A possible explanation is that high temperatures could promote the degradation reaction of polysaccharide, resulting the decrease of the polysaccharide extraction yield (Zhao et al., 2015).This tendency is in good agreement with other previous study (Xu et al., 2016). As shown in Fig. 3C, MHP yield increased as the extraction time extended from 20 min to 28 min and then sharply decreased. This situation may be due to the heating effect, and overexposure to ultrasound treatment for longer extraction time, which caused the decomposition of polysaccharides during the extension in the extraction time (Ying et al., 2011). Liu et al. (2009) also found that the extraction yield of *Agaricus blazei* polysaccharide started to decrease upon extended extraction times. The results illustrated in Fig. 3D suggested the

Table 2
Analysis of variance for response surface quadratic model (full empirical model) using high-pressure ultrasonic-assisted extraction (HUAE) at three-level ratio of water to raw material (X_1), ultrasonic power (X_2), extraction temperature (X_3) and extraction time (X_4).

Source	SS	DF	MS	*F*-value	*P*-value	
Model	25.48	14	1.82	137.20	< 0.0001	Significant
X_1	0.25	1	0.25	19.02	0.0007	Significant
X_2	0.002408	1	0.002408	0.18	0.6765	Not significant
X_3	0.46	1	0.46	34.40	< 0.0001	Significant
X_4	0.010	1	0.010	0.77	0.3952	Not significant
X_1X_2	0.017	1	0.017	1.27	0.2780	Not significant
X_1X_3	0.048	1	0.048	3.65	0.0768	Not significant
X_1X_4	0.59	1	0.59	44.70	< 0.0001	Significant
X_2X_3	0.0009	1	0.0009	0.068	0.7983	Not significant
X_2X_4	0.48	1	0.48	36.41	< 0.0001	Significant
X_3X_4	0.0036	1	0.0036	0.27	0.6105	Not significant
X_{12}	6.23	1	6.23	469.54	< 0.0001	Significant
X_{22}	4.62	1	4.62	348.05	< 0.0001	Significant
X_{32}	16.76	1	16.76	1263.44	< 0.0001	Significant
X_{42}	7.37	1	7.37	555.84	< 0.0001	Significant
Residual	0.19	14	0.013			
Lack of fit	0.16	10	0.016	2.44	0.2018	Not significant
Pure error	0.026	4	0.00653			
Cor. total	25.67	28				
R^2	0.9928					
Adj-R^2	0.9855					
Pred-R^2	0.9626					
Adeq precision	36.67					
C.V.%	1.56					

Note: SS denotes sum of squares; DF denotes degree of freedom; MS denotes mean square.

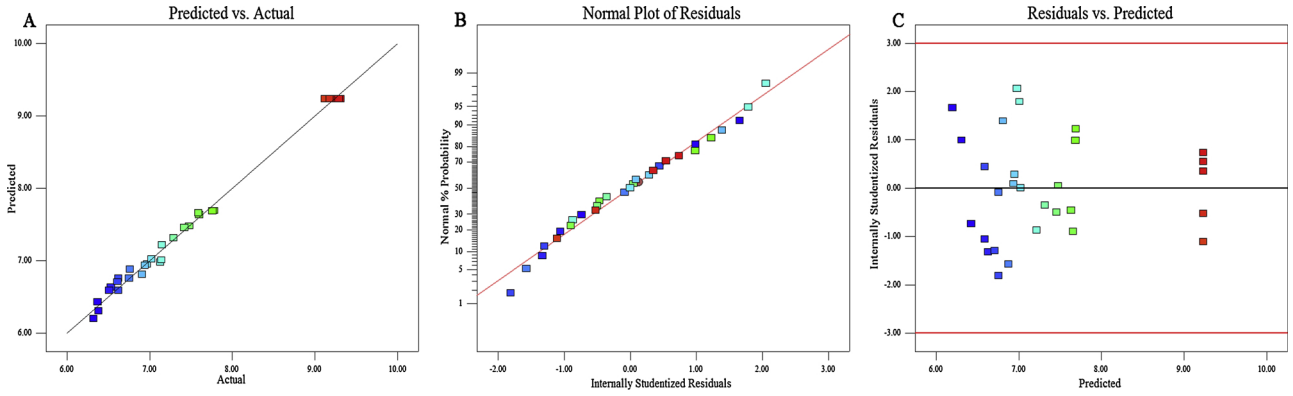

Fig. 2. Actual extraction yield vs. the predicted extraction yield under optimum extraction conditions (A); Plot of normal probability of internally studentized residuals (B); Plot of internally studentized residuals versus predicted response (C).

maximum MHP yield was achieved at 295 W and 69 °C, respectively. The interactions between ultrasonic power and extraction time were significant according to the 3D surface plots (Fig. 3E). MHP yield was found to increase as ultrasonic power and extraction time increased from 250 to 305 W and from 20 to 28 min, respectively. Moreover, a gradual increase in MHP yield was noticed as the extraction time extended from 20 min to 29 min and slow decrease was observed with the extension of extraction time over the range 29–40 min.

In accordance with the predictive regression equation and the response in variable perturbation observed in the 3D surface contour plots, the calculated conditions for the MHP extraction were as follows: water to raw material ratio, 28.97 mL/g; ultrasonic power, 303.47 W; extraction temperature, 69.65 °C; and extraction time, 28.58 min. Consequently, experimental parameters were set as follows: water to raw material ratio of 29 mL/g, ultrasonic power of 300 W, extraction temperature of 70 °C and extraction time of 28 min. Under these optimal conditions, the extraction yield of MHP was 9.41 ± 0.53% (n = 6), consistent with the prediction from the model, demonstrating that the model was reliable and effective for the prediction of MHP extraction.

3.2. Chemical analysis of MHP

The main chemical composition of MHP is listed in Table 4. The content of neutral sugar in MHP was 69.09%, similar to that previously reported for polysaccharides from the other *Mentha* species like *Mentha piperita* (70.48%) (Liu et al., 2014b). MHP was found to contain 3.89% uronic acid, indicating that MHP is an acidic heteropolysaccharide; however, the uronic acid value of MHP was lower than that of acid polysaccharides obtained from *M. piperita* (8.96%) (Liu et al., 2014b). Additionally, MHP exhibited a relative high protein content (7.97%), indicating that polysaccharide–protein complexes still resided in the extract. We propose that this residual protein content is due to protein conjugation to the MHP, as the free proteins were removed via the Sevag method. Previously reported research revealed that the functional and rheological properties of polysaccharides could be associated with their proteins (Wang et al., 2018). Consequently, we hypothesize that the MHP possessing 7.97% of protein may display functional properties related to those of the incorporated proteins. However, MHP was not found contain polyphenol and flavonoid. The monosaccharide composition of MHP is depicted in Fig. S1A (in Supplemental material) and Table 4. Analysis revealed MHP to be a heteropolysaccharide

Table 3
Analysis of variance for the truncated model using high-pressure ultrasonic-assisted extraction (HUAE) at three-level ratio of water to raw material (X_1), ultrasonic power (X_2), extraction temperature (X_3) and extraction time (X_4).

Source	SS	DF	MS	*F*-value	*P*-value	
Model	25.40	8	3.17	236.80	< 0.0001	Significant
X_1	0.25	1	0.25	18.82	0.0007	Significant
X_3	0.46	1	0.46	34.04	< 0.0001	Significant
X_1X_4	0.59	1	0.59	44.23	< 0.0001	Significant
X_2X_4	0.48	1	0.48	36.03	< 0.0001	Significant
X_{12}	6.23	1	6.23	464.60	< 0.0001	Significant
X_{22}	4.62	1	4.62	344.38	< 0.0001	Significant
X_{32}	16.76	1	16.76	1250.13	< 0.0001	Significant
X_{42}	7.37	1	7.37	549.98	< 0.0001	Significant
Residual	0.27	20	0.013			
Lack of fit	0.24	16	0.015	2.32	0.2163	Not significant
Pure error	0.026	4	0.00653			
Cor. total	25.67	28				
R^2	0.9896					
Adj-R^2	0.9854					
Pred-R^2	0.9744					
Adeq precision	45.383					
C.V.%	1.57					

Note: SS denotes sum of squares; DF denotes degree of freedom; MS denotes mean square.

Table 4
Chemical composition and monosaccharide composition of MHP.

Chemical composition (%, g/g)	MHP
Neutral sugar	69.09 ± 0.81
Protein	7.97 ± 0.42
Uronic acid	3.89 ± 0.14
Moisture	5.46 ± 0.32
Total polyphenol	N.D.
Total flavonoid	N.D.
Monosaccharide composition (molar%)	
Mannose	2.13 ± 0.18
Rhamnose	0.89 ± 0.04
Glucose	39.30 ± 0.16
Galactose	44.85 ± 2.99
Arabinose	7.89 ± 0.44
Glucuronic acid	1.14 ± 0.13
Galacturonic acid	3.79 ± 0.09

N.D.: Not detectable or lower than the limit of quantification.
Values are given as mean ± SD (standard deviation) from triplicate determinations.

consisting of seven types of monosaccharides including Man, Rha, GlcA, GalA, Glc, Gal, and Ara with molar percentages of 2.13, 0.89, 1.14, 3.79, 39.3, 44.85, and 7.89%, respectively. Therefore, Gal and Glc are the dominant monosaccharides in MHP. The monosaccharide composition of MHP determined through this study diverges significantly from the reported composition of *M. piperita*, which consisted of only five monosaccharides including GlcA, GalA, Glc, Gal, and Ara (Liu et al., 2014b).

3.3. Molecular weight of MHP

The molecular weight (M_w) distribution of MHP was measured using HPLC-RI; the resultant chromatograph is illustrated in Fig. S1B (see Supplemental material). Three adsorption peaks observed in the HPGPC curve of MHP suggested heterogeneity of the sample with three major components. Based on a calibration curve prepared with dextran standards, the three species of MHP with M_ws of 59.58 kDa, 35.58 kDa and 12.45 kDa were present in relative ratios of 66.20%, 11.60% and 22.20%, respectively. The M_ws of the species in MHP were considerably larger than those obtained from *M. piperita*, which contained only two major fractions with M_ws of 2.843 and 1.139 kDa (Liu et al., 2014b). Low molecular weight polysaccharides have been found to exhibit excellent water-solubility and bioactive properties (Chen et al., 2004); as such, we pursued characterization of the functional properties and evaluation of the antioxidant activities of the isolated MHP, which will be described in subsequent sections of this report.

3.4. FT-IR spectrum of MHP

The result of the FT-IR spectrum of MHP is presented in Fig. 4A. The broadband in the region of 3392 cm^{-1}belongs to stretching vibration of O—H, while the weak peak around 2932.6 cm^{-1}represents stretching vibration of C—H. Absorption peaks at 1603.9 and 1413.7 $cm^{-1}$are

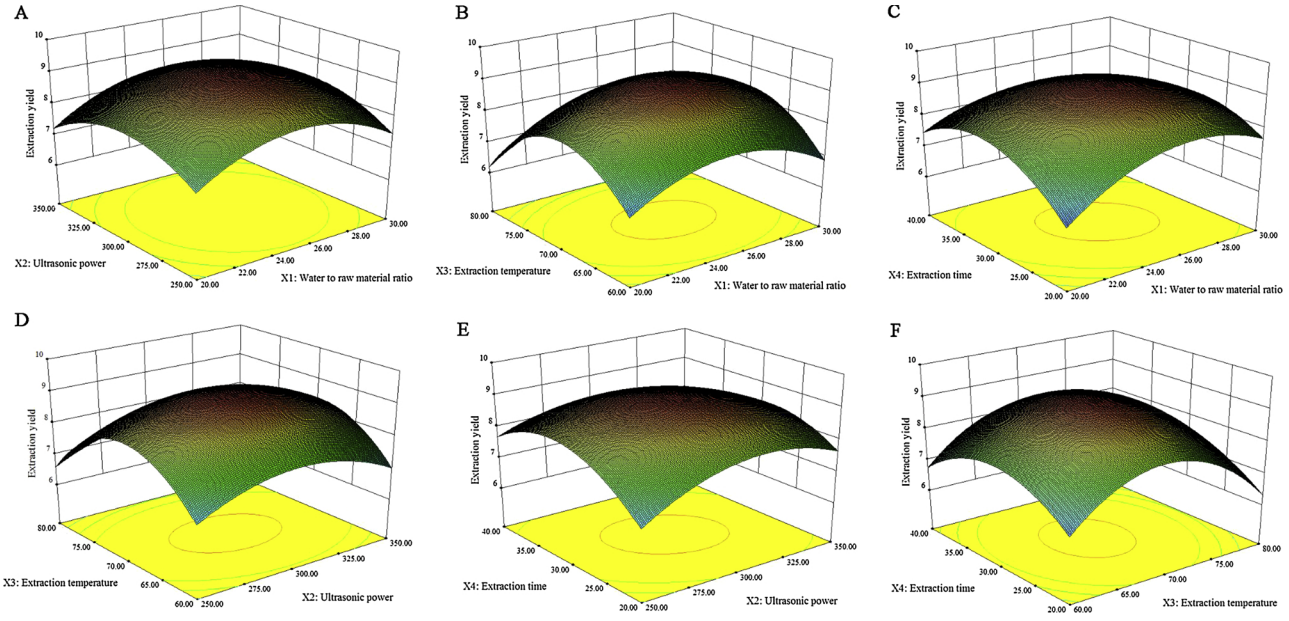

Fig. 3. Response surface plots for the interaction effect (A) ultrasonic power and ratio of water to raw material; (B) ratio of water to raw material and extraction temperature; (C) ratio of water to raw material and extraction time; (D) ultrasonic power and extraction temperature; (E) ultrasonic power and extraction time; (F) extraction temperature and extraction time.

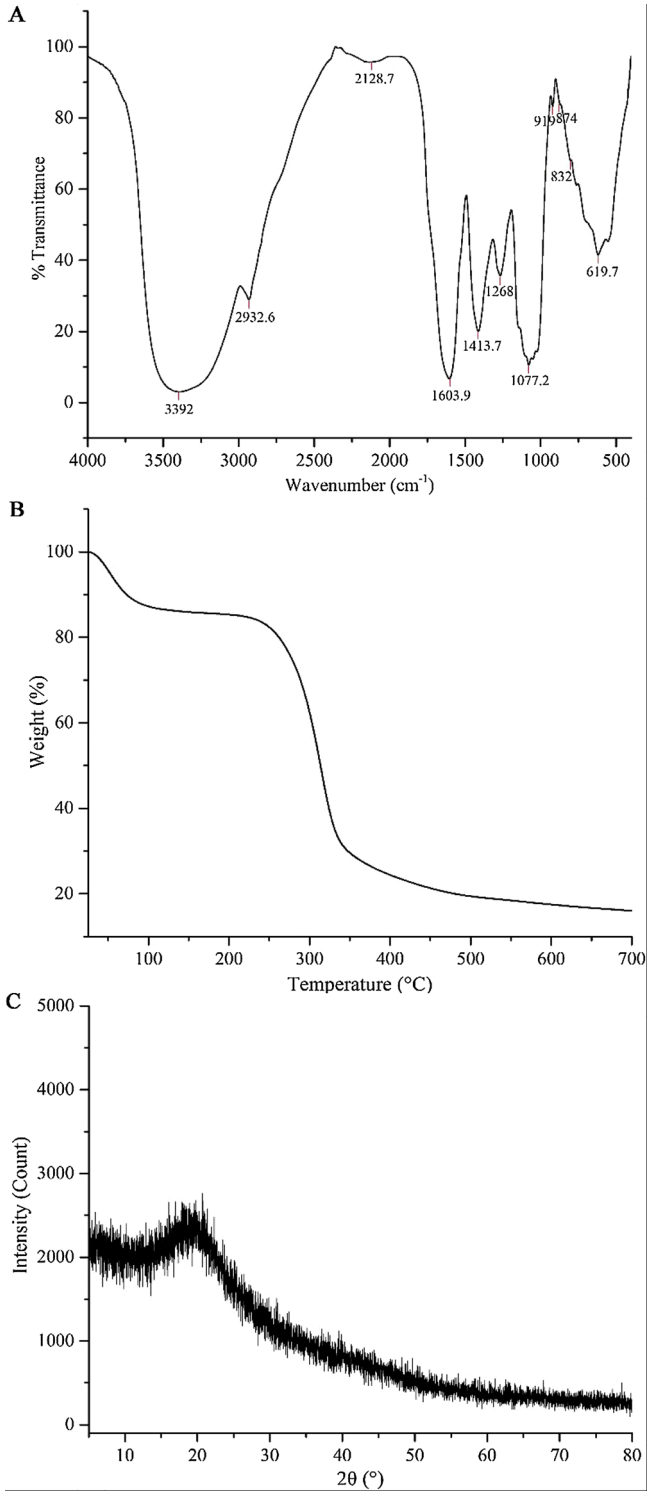

Fig. 4. The FT-IR spectrum (A), TGA thermogram (B), and X-ray diffraction pattern (C) of MHP.

assigned to be the C═O bending and C—H bending, respectively. The signal observed at 1268 cm^{-1} is attributed to C − O stretching in the ring, and the peak at 1077.2 cm^{-1} to the glycosidic linkage C − O—C stretching vibration. In addition, three characteristic absorptions at 919 cm^{-1}, 874 cm^{-1} and 832 cm^{-1} indicate the possible presence of both α- and β-pyranose in MHP.

3.5. Thermal characteristic

The application of polysaccharides in the food industry is depended on thermal properties such as heat flow rate. Generally, thermal stability of polysaccharides is predicated on their structural and functional group variations; this property is typically assessed using thermogravimetric analysis (TGA). The TGA curve of MHP, presented in Fig. 4B, shows a three-step degradation pattern. The first mass loss noted by TGA, which we attribute to the loss of water from the sample, occurs over the temperature range of 25 °C to 120 °C A more significant mass loss is then observed in the temperature range 220–520 °C, which is attributed to the depolymerisation of the polysaccharide structure. Little to no change in polysaccharide mass is observed when the temperature continues to increase. The residual mass of MHP at the end of TGA was approximately 17% of the original mass. The above results demonstrated a chemical stability of MHP in the temperature range of 20 °C to 220 °C.

3.6. X-ray (XRD) diffraction

X-ray diffraction is a powerful analytical tool employed to evaluate the crystalline characteristics of the polysaccharides, which can predict their various properties like flexibility, swelling, solubility and other physical properties. A low overall crystallinity was found from the XRD pattern of MHP presented in Fig. 4C. The crystalline region seen at the angle (2θ) 20.92 indicates MHP is semi-crystalline polymers. Similar crystalline region of polysaccharides extracted from potato peel waste was reported by Jeddou et al. (2016).

3.7. Functional properties

3.7.1. Water holding capacity (WHC) and oil holding capacity (OHC)

High water holding capacity is a favorable property for food applications as materials with a high WHC could be used as stabilizers, gelling agents and texture modifiers. The WHC of MHP was measured as 1.23 ± 0.04 g water/g, similar to that reported for water soluble polysaccharides extracted from pistachios (PWSP) (1.46 ± 0.62 g water/g) (Sila et al., 2014). On the other hand, the WHC of MHP was lower than that of polysaccharides derived from some other plant-based materials, such as almond (1.95 ± 0.10 g water/g) (Sila et al., 2014) and potato peel (4.097 ± 0.537 g water/g) (Jeddou et al., 2016).

The oil holding capacity of polysaccharide can be used as a predictive measure of adsorption of organic compounds to the surface of a material containing these polysaccharides. The OHC of MHP was computed as 4.46 ± 0.11 g oil/g, higher than that of the polysaccharides derived from *Rosa roxburghii Tratt* fruit (3.29 ± 0.38 g oil/g) (Wang et al., 2018) and watermelon rinds (4 ± 0.1 g oil/g) (Romdhane et al., 2017), but lower than that of polysaccharides obtained from pistachios (8.48 ± 1.59 g oil/g) (Sila et al., 2014). The relatively high OHC of MHP suggests a potential for use as a stabilizer in high-fat foods.

3.7.2. Foaming qualities

Foaming agents in food formulations stabilize the dispersion of gas throughout a food substance, for instance, in the airness of ice cream and milkshakes. Consequently, the foaming qualities of MHP have larger implications in its application in food technology as a foaming agent. The foaming capacity (FC) and foaming stability (FS) of MHP were examined at various concentrations (1%, 2%, 3%, 4% and 6%; w/v), and the results depicted in Fig. 5A. While MHP can achieve a slight foaming under low concentrations (1–2%), the resultant foam was unstable and largely dissipated within half an hour. However, the foaming qualities improved with increasing in MHP concentration. We propose that the observed reinforcement of foaming qualities is probably attributed to an increased ability of MHP to form a network at higher concentrations, thus stabilizing the interfacial film. Indeed, at

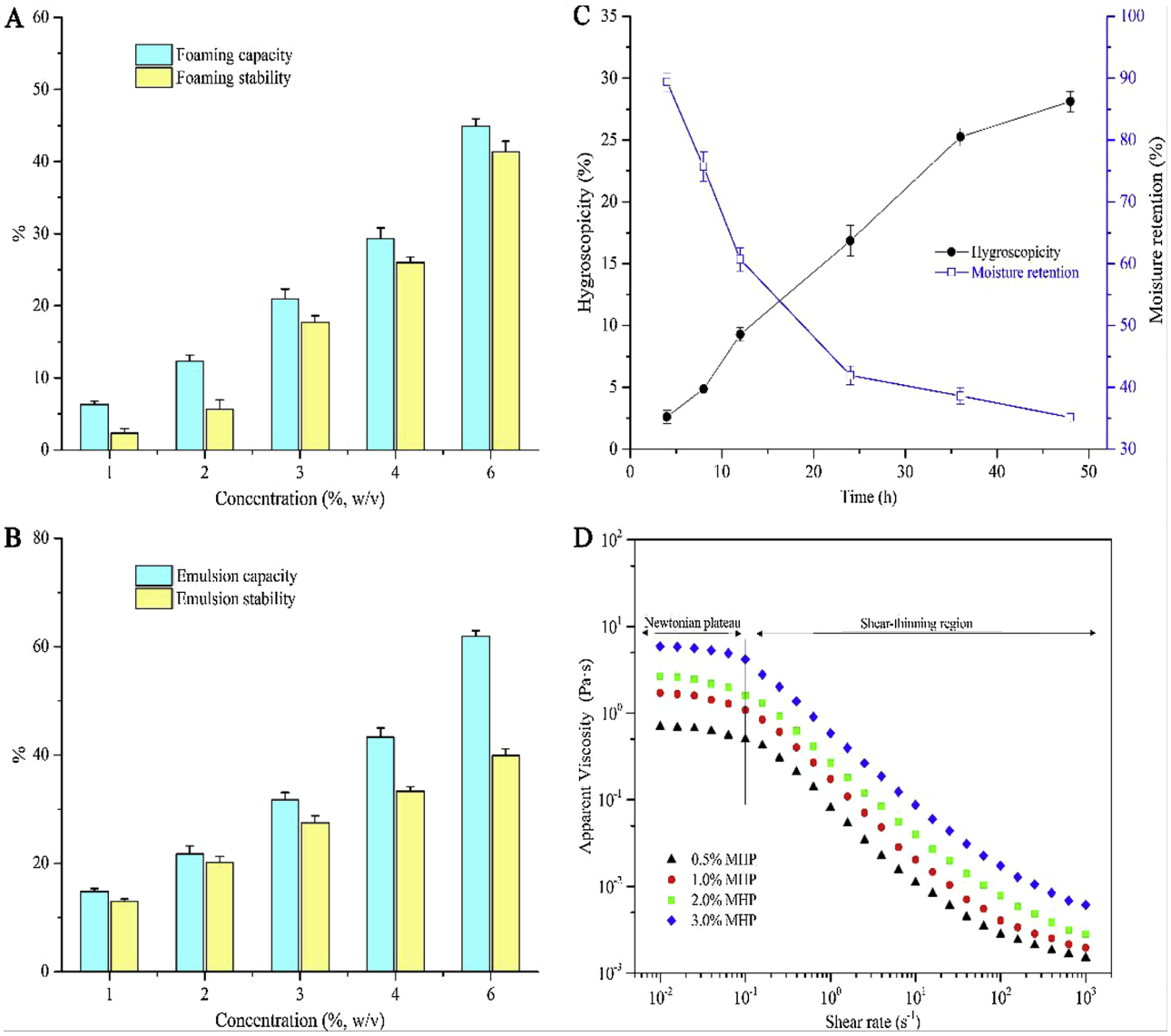

Fig. 5. (A) Foaming properties and (B) emulsifying properties of MHP measured at different concentrations; (C) Hygroscopicity and moisture retention of MHP. Each value is the means ± standard deviation (SD) of triplicate measurements. (D) Dependence of the apparent viscosity on the shear rate at different MHP concentrations. Steady-shear flow behavior were carried out at 25 °C.

concentrations of 4% and 6% MHP, the FCs were 29.28% and 44.92%, respectively. Moreover, after 30 min, minimal reduction of foam volume was observed at these concentrations. The observed FC and FS values for 4% and 6% MHP solutions suggest the potential of MHP for use as a foaming agent in food formulations.

3.7.3. Emulsion properties

Literature reports have suggested that the emulsion capacity (EC) and emulsion stability (ES) of polysaccharides are largely a function of the molecular composition, both of the composite sugar molecules and hydrophobic proteins, or of the rheological characteristics of the polysaccharides (Funami et al., 2011). The EC and ES of MHP at different concentrations (1%, 2%, 3%, 4% and 6%; w/v) are displayed graphically in Fig. 5B. The EC and ES values increase with the increasing MHP concentration. An exceptional EC of 62.1% is achieved with an MHP concentration of 6%, suggesting the applicability of MHP as an emulsifiers in food products.

3.7.4. Hygroscopicity and moisture retention analysis

As can be observed in Fig. 5C, the hygroscopicity of MHP significantly increases with the extension of storage time over the range 4–48 h. Conversely, moisture retention sharply decreases with the increasing of storage time. While the hygroscopicity and moisture retention of MHP (28.11% and 35.14%) are lower than that reported for glycerin (57.96% and 41.97%) (Zhu et al., 2017), MHP exhibits substantial hygroscopicity and a relatively strong moisture retention capacity. The hygroscopicity and moisture retention properties of MHP indicate that this polysaccharides may be used as a supplement in cosmetics.

3.8. Rheological properties

Fig. 5D depicts the rheological behavior of MHP in terms of apparent viscosity (η) *vs.* shear rate ($\dot{\gamma}$) across the different MHP concentrations (0.5, 1, 2, 3%, w/w). All samples exhibited a Newtonian plateau and a shear-thinning regime with increasing shear rates. The Newtonian plateau represents the region with low shear rates, where the apparent viscosity remains constant, indicating an equilibrium between the rate of molecular disentanglement and re-entanglement. In contrast, a decrease in apparent viscosity is observed as the shear rate

Table 5
Cross, Carreau, and Power-law models parameters at different MHP concentrations.

MHP (%)	Cross model fitting parameters					Carreau model fitting parameters					Power-law model fitting parameters[a]		
	a(s)	d	η_0(Pa·s)	η_∞(Pa·s)	R^2	c(s)	p	η_0(Pa·s)	η_∞(Pa·s)	R^2	k(Pa·s^n)	n	R^2
0.5	8.181	1.005	0.824	0.002	0.998	9.944	0.070	0.681	0.002	0.999	0.102	0.279	0.993
1	10.375	1.000	2.020	0.002	0.993	11.339	0.063	1.635	0.002	0.997	0.195	0.239	0.995
2	13.849	0.909	3.426	0.002	0.999	13.955	0.147	2.590	0.002	0.997	0.310	0.202	0.992
3	14.128	0.917	7.971	0.005	0.998	14.268	0.168	6.044	0.005	0.999	0.620	0.173	0.999

[a] Power-law model parameters for shear rates greater than 0.1/s at different MHP concentrations.

increase beyond a certain threshold in shear-thinning regime due to a reduced rate of entanglement (Guo et al., 2017). Even if the Newtonian behavior was noticed at lower shear rates, MHP clearly exhibits significant non-Newtonian pseudoplastic behaviour.

Parameters pertaining to flow behavior indices of the MHP solutions were analyzed by computed the Cross (Eq. (8)) and Carreau (Eq. (9)) models for low shear rates, and to the Power-law (Eq. (10)) model at high shear rates (> 0.1/s); the data is presented in Table 5. By comparing the regression coefficients (R^2) of the models, a better correlation was observed using the Carreau model than the Cross model, suggesting the Carreau model is better suited to describing the rheological characteristics of the MHP solutions ($R^2 \geq 0.997$). Moreover, a good correlation is also observed between the Power-law model and the experimental values for viscosity ($R^2 \geq 0.993$). Evaluating the viscosity, it was noted that the (η_0) increased from 0.681 to 6.044 Pa·s, and c increased from 9.944 to 14.268 s with increasing MHP concentration. Additionally, the rate index p increased (from 0.070 to 0.168) when the concentration of MHP increased from 0.5% to 3.0%. For a Newtonian solution, p will be 0; however, as an increase in shear thinning is observed, p will approach unity. As described above, the apparent viscosities in the MHP solutions were affected by concentration and shear rate, with a positive correlation to concentration and an inverse relationship with shear rate. The MHP demonstrated a pseudoplastic behavior when the values of the flow index (n) for Power-law model

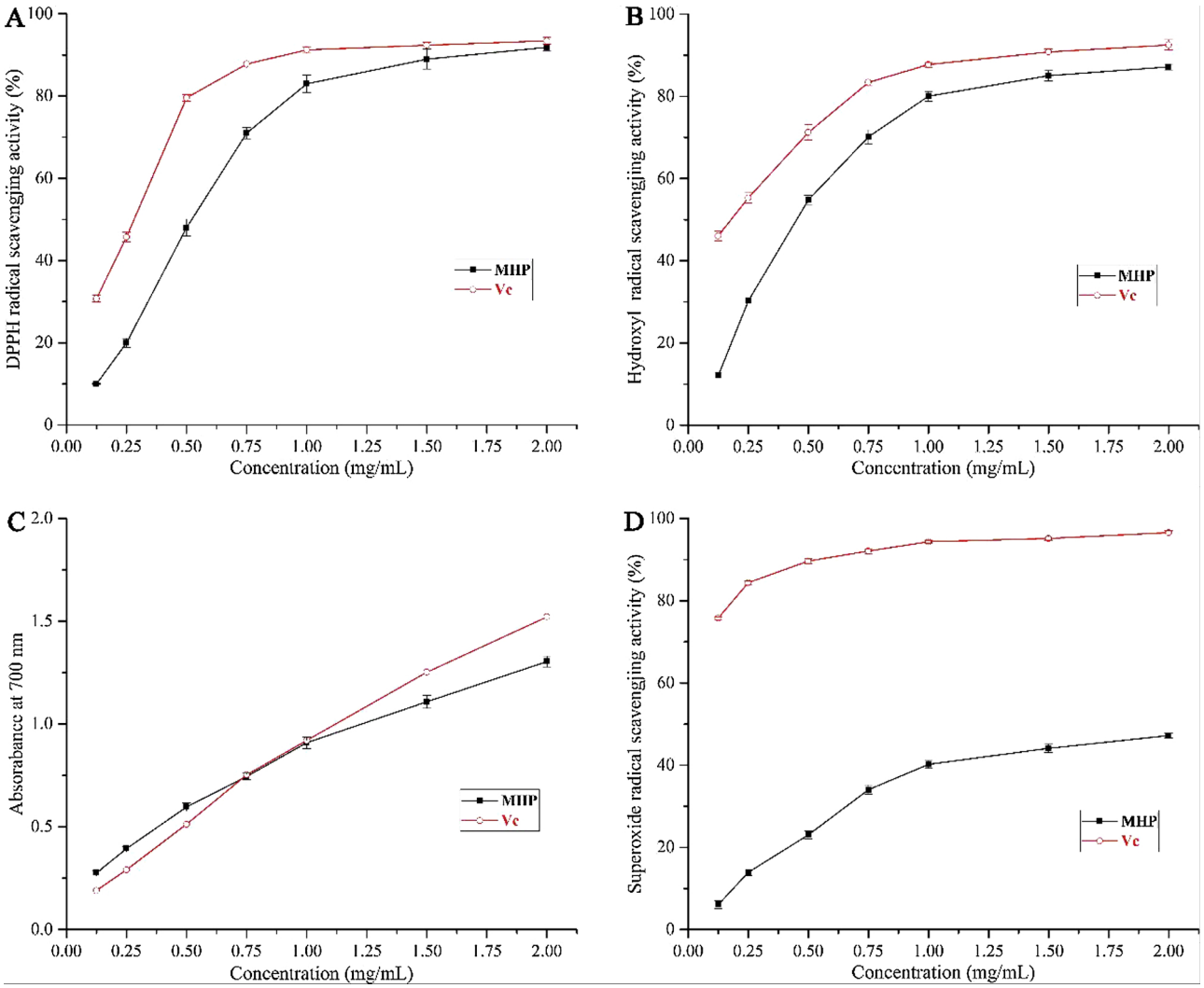

Fig. 6. Antioxidant activities of MHP at different concentrations: (A) DPPH radical scavenging activity; (B) Hydroxyl radical scavenging activity; (C) Reducing power; (D) Superoxide radical scavenging activity. Vc was used as the positive control. Each value is the means ± standard deviation (SD) of triplicate measurements.

were less than 1 in all samples (Table 5). A higher value of k is observed with higher MHP concentrations, further confirming that apparent viscosity increases with increasing MHP concentration.

3.9. Antioxidant activity of MHP

3.9.1. DPPH radical scavenging activity

As shown in Fig. 6A, MHP exhibited noticeable scavenging activity toward DPPH radical in a concentration-dependent manner. It was found that the DPPH radical scavenging activity (y) of MHP has a quadratic concentration (x)-dependent pattern ($p < 0.05$) and the quadratic equation is $y = -38.92x^2 + 126.23x - 5.23$ ($R^2 = 0.997$). The scavenging rate of MHP was 20.21% at 0.25 mg/mL; the scavenging rate activity increases up to 91.88% at 2 mg/mL. The scavenging activity of MHP, which exhibits an inhibitory concentration (IC_{50}) of 0.476 mg/mL, was similar to that of the positive control of Vc (IC_{50} = 0.232 mg/mL), indicating significant DPPH radical scavenging activity of MHP and that this polysaccharides can be considered an effective free radical inhibitor.

3.9.2. Hydroxyl radical scavenging activity

The results of hydroxyl scavenging experiments displayed in Fig. 6B yield a quadratic relationship between the scavenging ability (y) of MHP and MHP concentration (x) ($p < 0.05$), which can be described by the quadratic equation: $y = -37.77x^2 + 118.77x - 0.57$ ($R^2 = 0.986$). Although MHP has a higher IC_{50} value (0.476 mg/mL) than that of the positive control Vc (0.172 mg/mL), the maximum scavenging ability of MHP was only 94.20% that of Vc. These results demonstrate the hydroxyl scavenging capability of MHP and suggest its potential for use as a potent hydroxyl radical scavenger.

3.9.3. Ferric reducing power

As illustrated in Fig. 6C, the ferric reducing power (y) of MHP exhibits a linear relationship with MHP concentration (x) ($p < 0.05$), described by the linear equation: $y = 0.579x + 0.248$ ($R^2 = 0.966$). For concentrations ranging from 0.125 to 0.75 mg/mL, the reducing power of MHP was greater than that of Vc, but lower than that of Vc for concentrations exceeding 1.0 mg/mL. Notably, the reducing power of MHP reached 1.304 at the concentration of 2.0 mg/mL. The result of this test suggested good electron and hydrogen donor capabilities for MHP, to act as a catalyst for the termination of radical chain reactions.

3.9.4. Superoxide radical scavenging activity

Testing the superoxide radical scavenging activity (y) of MHP revealed a quadratic relationship with MHP concentration (x) ($p < 0.05$) of the form: $y = -15.40x^2 + 53.86x + 0.70$ ($R^2 = 0.991$) (Fig. 6D). The maximum scavenging rate of MHP at a concentration of 2.0 mg/mL was 47.20%, approximately half the capacity of Vc at the same concentration. Moreover, the IC_{50} value of MHP (1.77 mg/mL) was significantly higher than that of Vc (0.029 mg/mL). These results indicate a weak superoxide radical scavenging activity for MHP.

4. Conclusion

In the foregoing work, an efficient HUAE method was applied to extract polysaccharides from *M. haplocalyx*. Based on the RSM, the optimal HUAE conditions were identified as an ultrasonic power of 300 W, a temperature of 70 °C, an extraction time of 28 min, and a water to raw material ratio of 29 mL/g. Under these conditions, an MHP yield of 9.41 ± 0.53% was achieved. Structural analysis of MHP revealed a composition of Man, Rha, GlcA, GalA, Glc, Gal and Ara, with an average molecular weight of 59.58 kDa for its major species. Thermal analysis revealed a good thermal stability of MHP. Moreover, MHP exhibited interesting oil-holding capacity, foaming qualities, emulsion capacity, potential hygroscopicity, and moisture retention capacity. The MHP solution displayed shear-thinning flow behavior, well fitted by the Carreau and Power-law models. In addition, dose-dependent antioxidant activity of MHP was indicated by an *in vitro* assay against DPPH and hydroxyl radical. The physical properties and antioxidant behavior of MHP suggest the potential for its use as an additive in the food, pharmaceutical or cosmetic industries. The results of this study demonstrate a new and highly efficient method for extraction, and suggest several possible applications for the polysaccharides derived from *M. haplocalyx*.

Acknowledgement

This work was supported financially by the Key Program for International S&T Cooperation Projects of China (No. 2016YFE0130600).

Appendix A. Supplementary data

Supplementary material related to this article can be found, in the online version, at doi:https://doi.org/10.1016/j.indcrop.2018.12.086.

References

Bi, H., Gao, T., Li, Z., Ji, L., Yang, W., Jeff, I.B., et al., 2013. Structural elucidation and antioxidant activity of a water-soluble polysaccharide from the fruit bodies of *Bulgaria inquinans* (fries). Food Chem. 138 (2–3), 1470–1475.

Blumenkrantz, N., Asboe-Hansen, G., 1973. New method for quantitative determination of uronic acids. Anal. Biochem. 54 (2), 484–489.

Cao, G., Shan, Q., Li, X., Cong, X., Zhang, Y., Cai, H., et al., 2011. Analysis of fresh *Mentha haplocalyx* volatile components by comprehensive two-dimensional gas chromatography and high-resolution time-of-flight mass spectrometry. Analyst 136 (22), 4653–4661.

Chen, H., Zhang, M., Xie, B., 2004. Quantification of uronic acids in tea polysaccharide conjugates and their antioxidant properties. J. Agric. Food Chem. 52 (11), 3333–3336.

Chen, R., Jin, C., Li, H., Liu, Z., Lu, J., Li, S., et al., 2014. Ultrahigh pressure extraction of polysaccharides from *Cordyceps militaris*, and evaluation of antioxidant activity. Sep. Purif. Technol. 134, 90–99.

Chen, C., Zhang, B., Huang, Q., Fu, X., Liu, R.H., 2017a. Microwave-assisted extraction of polysaccharides from *Moringa oleifera* Lam. leaves: characterization and hypoglycemic activity. Ind. Crops Prod. 100, 1–11.

Chen, X., Zhang, S., Xuan, Z., Ge, D., Chen, X., Zhang, J., et al., 2017b. The phenolic fraction of *Mentha haplocalyx* and its constituent linarin ameliorate inflammatory response through inactivation of NF-κB and MAPKs in lipopolysaccharide-induced RAW264.7 cells. Molecules 22 (5), 811.

Chen, G., Chen, K., Zhang, R., Chen, X., Hu, P., Kan, J., 2018a. Polysaccharides from bamboo shoots processing by-products: new insight into extraction and characterization. Food Chem. 245, 1113–1123.

Chen, G., Bu, F., Chen, X., Li, C., Wang, S., Kan, J., 2018b. Ultrasonic extraction, structural characterization, physicochemical properties and antioxidant activities of polysaccharides from bamboo shoots (*Chimonobambusa quadrangularis*) processing by-products. Int. J. Biol. Macromol. 112, 656–666.

Dong, C.X., Hayashi, K., Mizukoshi, Y., Lee, J.B., Hayashi, T., 2011. Structures of acidic polysaccharides from *Basella rubra* L. and their antiviral effects. Carbohydr. Polym. 84 (3), 1084–1092.

Dong, W., Ni, Y., Kokot, S., 2015. Differentiation of mint (*Mentha haplocalyx* Briq.) from different regions in china using gas and liquid chromatography. J. Sep. Sci. 38 (3), 402–409.

Dubois, M., Gilles, K.A., Hamilton, J.K., Rebers, P.A., Smith, F., 1956. Colorimetric method for determination of sugars and related substances. Anal. Chem. 28 (3), 350–356.

Funami, T., Nakauma, M., Ishihara, S., Tanaka, R., Inoue, T., Phillips, G.O., 2011. Structural modifications of sugar beet pectin and the relationship of structure to functionality. Food Hydrocoll. 25 (2), 221–229.

Gan, C.Y., Latiff, A.A., 2011. Extraction of antioxidant pectic-polysaccharide from mangosteen (*Garcinia mangostana*) rind: optimization using response surface methodology. Carbohydr. Polym. 83 (2), 600–607.

González-Centeno, M.R., Knoerzer, K., Sabarez, H., Simal, S., Rosselló, C., Femenia, A., 2014. Effect of acoustic frequency and power density on the aqueous ultrasonic-assisted extraction of grape pomace (Vitis vinifera L.) – a response surface approach. Ultrason. Sonochem. 21, 2176–2184.

Guo, X., Shang, X., Zhou, X., Zhao, B., Zhang, J., 2017. Ultrasound-assisted extraction of polysaccharides from *Rhododendron aganniphum*: antioxidant activity and rheological properties. Ultrason. Sonochem. 38, 246–255.

He, S.D., Wang, X., Zhang, Y., Wang, J., Sun, H.J., Wang, J.H., et al., 2016. Isolation and prebiotic activity of water-soluble polysaccharides fractions from the bamboo shoots (*Phyllostachys praecox*). Carbohydr. Polym. 151, 295–304.

Jeddou, K.B., Chaari, F., Maktouf, S., Nouriellouz, O., Helbert, C.B., Ghorbel, R.E., 2016. Structural, functional, and antioxidant properties of water-soluble polysaccharides from potatoes peels. Food Chem. 205, 97–105.

Jia, Z.S., Tang, M.C., Wu, J.M., 1999. The determination of flavonoid contents in mulberry and their scavenging effects on superoxide radicals. Food Chem. 64, 555–559.
Liao, N., Zhong, J., Ye, X., Lu, S., Wang, W., Zhang, R., et al., 2015. Ultrasonic-assisted enzymatic extraction of polysaccharide from Corbicula fluminea: characterization and antioxidant activity. LWT-Food Sci. Technol. 60 (2), 1113–1121.
Liu, Y., Zhang, Y.H., Shi, R.B., 2005. Studies on the chemical constituents in herb of *Mentha haplocalyx*. China J. Chin. Matera Med. 30 (14), 1086–1088 (in Chinese).
Liu, J., Miao, S., Wen, X., Sun, Y., 2009. Optimization of polysaccharides (ABP) extraction from the fruiting bodies of *Agaricus blazei* Murill using response surface methodology (RSM). Carbohydr. Polym. 78 (4), 704–709.
Liu, Y., Wei, S., Liao, M., 2013. Optimization of ultrasonic extraction of phenolic compounds from *Euryale ferox* seed shells using response surface methodology. Ind. Crops Prod. 49 (4), 837–843.
Liu, J.L., Zheng, S.L., Fan, Q.J., Yuan, J.C., Yang, S.M., Kong, F.L., 2014a. Optimization of high-pressure ultrasonic-assisted simultaneous extraction of six major constituents from *Ligusticum chuanxiong* rhizome using response surface methodology. Molecules 19 (2), 1887–1911.
Liu, X., Sun, Z.L., Jia, A.R., Shi, Y.P., Li, R.H., Yang, P.M., 2014b. Extraction, preliminary characterization and evaluation of in vitro antitumor and antioxidant activities of polysaccharides from *Mentha piperita*. Int. J. Mol. Sci. 15 (9), 16302–16319.
Liu, J.L., Zheng, S.L., Fan, Q.J., Yuan, J.C., Yang, S.M., Kong, F.L., 2015. Optimisation of high-pressure ultrasonic-assisted extraction and antioxidant capacity of polysaccharides from the rhizome of *Ligusticum chuanxiong*. Int. J. Biol. Macromol. 76, 80–85.
Lou, X.W., Janssen, H.G., Cramers, C.A., 1997. Parameters affecting the accelerated solvent extraction of polymeric samples. Anal. Chem. 69 (8), 1598–1603.
McClements, D.J., Bai, L., Chung, C., 2017. Recent advances in the utilization of natural emulsifiers to form and stabilize emulsions. Annu. Rev. Food Sci. Technol. 8 (1), 205–236.
Mimica-Dukic, N., Bozin, B., 2008. *Mentha* L. species (Lamiaceae) as promising sources of bioactive secondary metabolites. Curr. Pharm. Des. 14 (29), 3141–3150.
Noshad, M., Mohebbi, M., Shahidi, F., Mortazavi, S.A., 2012. Multi-objective optimization of osmotic–ultrasonic pretreatments and hot-air drying of quince using response surface methodology. Food Bioproc. Technol. 5 (6), 2098–2110.
Park, Y.J., Baskar, T.B., Yeo, S.K., Arasu, M.V., Al-Dhabi, N.A., Lim, S.S., et al., 2016. Composition of volatile compounds and in vitro antimicrobial activity of nine *Mentha*, spp. Springerplus 5 (1), 1628.
Rezaei, A., Nasirpour, A., Tavanai, H., 2016. Fractionation and some physicochemical properties of almond gum (*Amygdalus communis* L.) exudates. Food Hydrocoll. 60, 461–469.
Romdhane, M.B., Haddar, A., Ghazala, I., Jeddou, K.B., Helbert, C.B., Ellouz-Chaabouni, S., 2017. Optimization of polysaccharides extraction from watermelon rinds: structure, functional and biological activities. Food Chem. 216, 355–364.
Sevag, M.G., Lackman, D.B., Smolens, J., 1938. The isolation of the components of streptococcal nucleoproteins in serologically active form. J. Biol. Chem. 124, 425–436.
She, G.M., Xu, C., Liu, B., 2012. New monocyclic monoterpenoid glycoside from mentha haplocalyx briq. Chem. Cent. J. 6, 37.
Sila, A., Bayar, N., Ghazala, I., Bougatef, A., Ellouz-Ghorbel, R., Ellouz-Chaabouni, S., 2014. Water-soluble polysaccharides from agro-industrial by-products: functional and biological properties. Int. J. Biol. Macromol. 69 (8), 236–243.
Sun, L., Zhou, Y., 2012. Immunomodulation and antitumor activities of different molecular-weight polysaccharides from *Porphyridium cruentum*. Carbohydr. Polym. 87 (2), 1206–1210.
Wang, L., Zhang, B., Xiao, J., Huang, Q., Li, C., Fu, X., 2018. Physicochemical, functional, and biological properties of water-soluble polysaccharides from *Rosa roxburghii* tratt fruit. Food Chem. 249, 127–135.
Wei, X.G., Dong, Y., Cui, Q.X., Zhang, G.L., 2003. GC-MS analysis of essential oil of the uncultivated *Mentha hapioealyx* Briq. Yantai Normal Univ. 19, 16–118 (in Chinese).
Wijesinghe, W.A., Jeon, Y.J., 2012. Enzyme-assistant extraction (EAE) of bioactive components: a useful approach for recovery of industrially important metabolites from seaweeds: a review. Fitoterapia 83 (1), 6–12.
Xu, Y., Cai, F., Yu, Z., Zhang, L., Li, X., Yang, Y., et al., 2016. Optimisation of pressurised water extraction of polysaccharides from blackcurrant and its antioxidant activity. Food Chem. 194, 650–658.
Yang, S., Jia, D., Yao, K., Liu, W., Li, Y., 2017. Synergy of box-behnken designs on the optimization of polysaccharide extraction from mulberry leaves. Ind. Crops Prod. 99, 70–78.
Yen, G.C., Hsieh, C.L., 1998. Antioxidant activity of extracts from Du-zhong (*Eucommia ulmoides*) toward various lipid peroxidation models in vitro. J. Agric. Food Chem. 46 (10), 3952–3957.
Ying, Z., Han, X., Li, J., 2011. Ultrasound-assisted extraction of polysaccharides from mulberry leaves. Food Chem. 127 (3), 1273–1279.
Zhao, Z.Y., Zhang, Q., Li, Y.F., Dong, L.L., Liu, S.L., 2015. Optimization of ultrasound extraction of *Alisma orientalis* polysaccharides by response surface methodology and their antioxidant activities. Carbohydr. Polym. 119, 101–109.
Zheng, W., Wang, S.Y., 2001. Antioxidant activity and phenolic compounds in selected herbs. J. Agric. Food Chem. 49 (11), 5165–5170.
Zhu, Z., Dong, F., Liu, X., Lv, Q., Ying, Y., Liu, F., et al., 2016. Effects of extraction methods on the yield, chemical structure and anti-tumor activity of polysaccharides from *Cordyceps gunnii* mycelia. Carbohydr. Polym. 140, 461–471.
Zhu, D.Y., Ma, Y.L., Wang, C.H., Wang, H., Ren, Y.F., Zhang, J.G., et al., 2017. Insights into physicochemical and functional properties of polysaccharides sequentially extracted from onion (*Allium cepa* L.). Int. J. Biol. Macromol. 105 (Pt. 1), 1192–1201.
Zor, T., Selinger, Z., 1996. Linearization of the Bradford protein assay increases its sensitivity: theoretical and experimental studies. Anal. Biochem. 236, 302–308.